



Tailoring surfaces of one-dimensional magnetophotonic crystals: Optical Tamm state and Faraday rotation

T. Goto,¹ A. V. Baryshev,^{1,2} M. Inoue,¹ A. V. Dorofeenko,³ A. M. Merzlikin,³ A. P. Vinogradov,³
A. A. Lisyansky,⁴ and A. B. Granovsky⁵

¹*Toyohashi University of Technology, Toyohashi 441-8580, Aichi, Japan*

²*Ioffe Physico-Technical Institute, St. Petersburg 194021, Russia*

³*Institute for Theoretical and Applied Electromagnetics, Moscow 125412, Russia*

⁴*Department of Physics, Queens College of the City University of New York, Flushing, New York 11367, USA*

⁵*Moscow State University, Moscow 119992, Russia*

(Received 19 November 2008; revised manuscript received 27 January 2009; published 4 March 2009)

We demonstrate that microscale tailoring of surfaces of magnetophotonic crystals provides an approach to engineer responses of known materials. In particular, we study states that are spatially localized at the interface between magnetophotonic and photonic crystals. Such states are an optical analog of the Tamm states long known in solid-state physics. The optical Tamm states are spectrally located inside band gaps and are associated with a sharp transmission peak in spectra of the system. Substantial enhancement of the Faraday rotation for the wavelength of the optical Tamm state is experimentally observed and attributed to strong light coupling to magnetic constituents of the magnetophotonic crystal. The experimental results are in excellent agreement with the theoretical predictions.

DOI: [10.1103/PhysRevB.79.125103](https://doi.org/10.1103/PhysRevB.79.125103)

PACS number(s): 78.20.Ls, 42.70.Qs, 42.25.Bs

I. INTRODUCTION

Up-to-date methods of microfabrication allow us to create inhomogeneous structures such as photonic crystals (PCs) with high accuracy. PCs with periodically modulated dielectric properties attract an ever-growing interest since they are finding various applications in nanoscale photonic devices.¹ Photonic band structures of PCs may have full band gaps, their spectra may exhibit localization or guiding of light by intentionally introduced defects, and electromagnetic waves may propagate at PC surfaces.^{2,3} Designing a microscopic distribution of fields inside the primitive cell of a PC allows for tuning light interaction with PC constituents made of active materials and for a significant change in their optical, magneto-optical, and other responses.⁴⁻¹⁹

The paradigm of the PCs and even the term “crystal” has been transferred into electrodynamics from solid-state physics where the behavior of electrons in a periodic system is well studied. It is the wave equation, which describes both the wave function and the electromagnetic wave, that underlines the common features of a crystal in solid-state physics and electrodynamics. Particularly, in the one-dimensional (1D) case, Schrödinger’s equation

$$-\frac{1}{2m} \frac{d^2\Psi}{dx^2} + [U(x) - E]\Psi = 0 \quad (1)$$

is identical with the electromagnetic wave equation describing a medium composed of isotropic materials

$$\frac{d^2\mathbf{E}}{dx^2} + k_0^2 \varepsilon(x) \mathbf{E} = 0. \quad (2)$$

In fact, if one makes the following substitutions:

$$-2m[U(x) - E] \rightarrow k_0^2 \varepsilon(x) \quad \text{and} \quad \Psi \rightarrow E, \quad (3)$$

then Eq. (1) turns into Eq. (2).²⁰ In the case of solid-state physics, $E > U(x)$ and $E < U(x)$ correspond to the propagation of electromagnetic waves in a medium with $\varepsilon(x) > 0$ and $\varepsilon(x) < 0$, respectively. The one-to-one correspondence between Eqs. (1) and (2) allows us to establish the mapping between solid-state physics and electrodynamics of PCs. Moreover, this correspondence allows us to transfer the well-known phenomena from solid-state physics into electrodynamics of PCs. Finally, this is the reason why many techniques that are fruitful in solid-state physics are applicable to problems in PCs.

It has been recently shown theoretically and experimentally in Ref. 21 that a boundary between two 1D PCs causes a localized state to appear.¹⁰⁻¹⁵ The frequency of such states is located inside the intersection of the band gaps of two PCs. The eigensolution $g(x)e^{ik_{\text{Bl}}x}$ inside a PC is the Bloch wave that consists of two factors—the exponential part $e^{ik_{\text{Bl}}x}$, where k_{Bl} is the Bloch wave number, and a periodic function $g(x)$. For the band-gap frequencies, the Bloch wave number k_{Bl} is an imaginary quantity; therefore the electromagnetic field decreases exponentially from interfaces of a PC and is still modulated by the $g(x)$ function. In the case of two adjoining PCs, two periodic g functions make it possible to satisfy the boundary conditions between two exponentially evanescent from the interface Bloch waves. This results in the arising of a state localized at the interface between two PCs.

A comparison of this state in PCs with Tamm²² and Shockley²³ surface states known in solid-state physics shows¹⁰⁻¹⁵ that the state observed in optical spectra is intrinsically closer to the Tamm state. In the work of Tamm,²² the local electron state appears at the boundary between a crystal and a medium characterized by a uniform potential U , when

the energy of the electron E is smaller than U . This state is located in the band gap of the crystal. The corresponding wave function, Ψ , exponentially decreases away from the boundary. For the electromagnetic case, one of the PCs plays the role of a conventional crystal, while the second PC provides a model potential $U > E$. This outlines the similarity between the Tamm state in electronic crystals and the optical Tamm state (OTS).

However, in spite of this similarity, OTSs are not direct analogs of the classical the Tamm states in terms of the one-to-one correspondence provided by the substitution, Eq. (3). The direct mapping of the Tamm structure onto the electrodynamics would be a system comprised of a PC and a medium with a negative permittivity adjoined to the PC. That is why one may expect an existence of a surface state in such a system. In fact, the existence of OTSs in such a system was theoretically predicted in Refs. 10–15. In this work, an observation of these states and a comparison between OTSs are presented for the different systems.

We have fabricated PCs with magnetic constituents in order to demonstrate the influence of the OTS on magneto-optical responses of the structures under study. It was experimentally found that (i) OTS causes an enhancement of the transmissivity and (ii) light with the wavelengths corresponding to the OTS is strongly coupled to magnetic constituents. This leads to a narrow sharp transmission peak to appear within band gaps and the Faraday rotation to be substantially enhanced. Data of experiments and theoretical results show excellent agreement.

II. SAMPLES AND EXPERIMENTAL DETAILS

The structures used in experiments were made to satisfy conditions for OTSs by using the approach reported in Ref. 10. Sample 1 was comprised of two adjoining 1D PCs deposited on a quartz substrate using ion-beam sputtering. The first PC was a dielectric multilayer composed of five pairs of $\text{Ta}_2\text{O}_5/\text{SiO}_2$ films with a Ta_2O_5 film at the end. The thicknesses of films were 94 nm (Ta_2O_5) and 138 nm (SiO_2). The second magnetic photonic crystal (MPC) was formed atop of PC 1. Films of bismuth-substituted yttrium garnet (Bi:YIG) were the magnetic constitutive elements of PC 2 comprising five repetitions of the Bi:YIG/ SiO_2 pair; the thicknesses of Bi:YIG and SiO_2 films were 86 and 138 nm, respectively. Each Bi:YIG film was annealed after its deposition in air at 700 °C for 15 min. The resultant structure was a quartz substrate/ Ta_2O_5 /($\text{SiO}_2/\text{Ta}_2\text{O}_5$)⁵/(Bi:YIG/ SiO_2)⁵ multilayer [Fig. 1(a)]. The parameters of the sample were chosen such that the OTS appeared at a wavelength of 800 nm, where Bi:YIG films exhibit a high transmittance and a satisfactory Faraday rotation. Sample 2 [Fig. 4(a)] was a quartz substrate/($\text{SiO}_2/\text{Bi:YIG}$)⁵/Au multilayer in which the thicknesses of layers were 125 nm (SiO_2), 83 nm (Bi:YIG), and 30 nm (Au). For the sputtered films, deviations of their thicknesses from desired values were less than 10%. Refractive indices of the materials involved in the work and used for simulations were taken from Refs. 24–26. For sample 2, the best-match calculated spectra were obtained for the Au film with $n=0.175$ and $k=4.9126$.

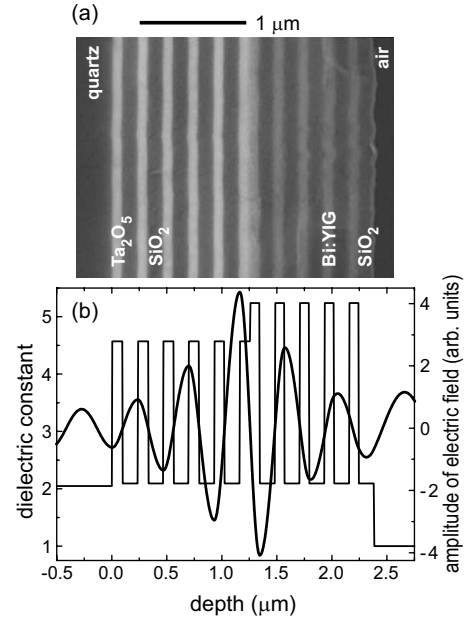


FIG. 1. (a) Scanning electron microscope image of sample 1, the system of two adjoining PCs. (b) Sketch of the spatial distribution of dielectric constants and the in-sample distribution of the electric field amplitude for the resonant wavelength.

Structural properties of the samples were evaluated using a Jeol JSM-6700 scanning electron microscope and energy dispersive x-ray spectroscopy. Optical responses were measured by a Shimadzu UV-3100PC spectrophotometer and an apparatus for magneto-optical studies (Neo Ark BH-M600VIR-FKR-TU). According to energy dispersive x-ray spectra and magneto-optical measurements, the annealing conditions were sufficient to obtain $\text{Bi}_1\text{Y}_2\text{Fe}_5\text{O}_{12}$ single garnet-phase polycrystalline (Bi:YIG) layers with the regular Faraday rotation. Transmission and Faraday rotation spectra were obtained with 5-nm spectral resolution (at normal incidence) for polarized collimated beams; the angular divergence was less than 1° , and the cross-sectional size of the light beam was about 2 mm^2 . To evaluate the Faraday rotation at extremely low intensities of the transmitted light (within the photonic band gap), a photon-counting mode with long acquisition intervals was used; the accuracy of analysis was 0.02° .

III. RESULTS AND DISCUSSION

Experimental transmission spectra of PC 1, PC 2, and combined sample 1 are shown in Fig. 2. One can see that each PC exhibits a band gap in the spectral range of 650–1000 nm, and there is a transmission maximum of 40% inside the stop band at 800 nm for the sample. For this wavelength, the distribution of the electric field amplitude within the sample is shown in Fig. 1(b). The amplitude is remarkably high at the interface between two PCs; it falls exponentially away from the interface. Such a distribution confirms the formation of the OTS. Note that all the maxima of the OTS amplitudes are spatially located within (or close to) the Bi:YIG layers. This also confirms that the electric field of the

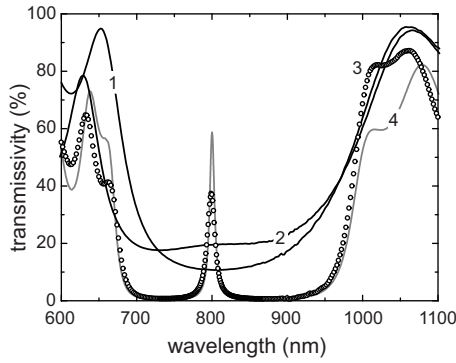


FIG. 2. Transmissivity of PC 1 and PC 2 alone are denoted by (1) and (2), respectively. Transmissivity of the system of adjoining PCs is shown by circles (3); its calculated spectrum is given by curve (4).

emerging wave with the wavelength of 800 nm is mostly concentrated in the Bi:YIG layers. Below, we demonstrate that the OTS provides strong optical coupling to the Bi:YIG layers, resulting in an enhanced magneto-optical response.

In order to verify that the peak shown in Fig. 2 is due to the OTS, magneto-optical spectra of the reference structure (PC 2) and of the sample were measured. According to the theoretical predictions, if one of the adjoining PCs is magnetic, an OTS should cause a substantial enhancement of the Faraday rotation.¹⁰ Experimental spectra are shown in Fig. 3. The Faraday rotation of PC 2 follows in the measured spectral range the ordinary monotonic response from the Bi:YIG constituent layers (black solid line). As for the combined sample, the Faraday rotation was -0.82° at the transmission peak of 800 nm, which was almost an order of magnitude larger than the value in PC 2 of -0.11° . The peak linewidths of in the transmission and Faraday rotation spectra were ≈ 10 nm.

Figures 4–6 show responses of sample 2. The behavior of the electric field amplitude distribution is similar to discussed above: (i) the amplitude is remarkably high at (and falls away from) the interface between the MPC and the Au film and (ii) the maxima of this distribution are located inside the Bi:YIG layers (Fig. 4). Transmission spectra of sample 2 and its constituents are plotted in Fig. 5. One can see that the OTS with the wavelength of 780 nm exists inside the band gap of the multilayer; the intensity of the peak was

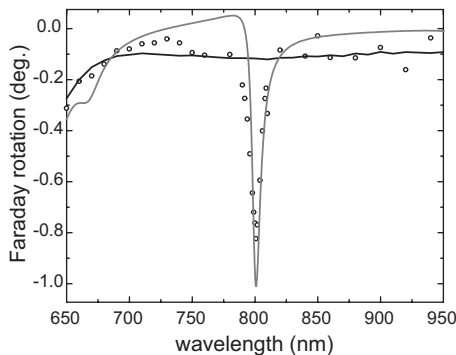


FIG. 3. Angle of Faraday rotation: PC 2 (black solid line), experimental (circles), and calculated (gray line) spectra of sample 1.

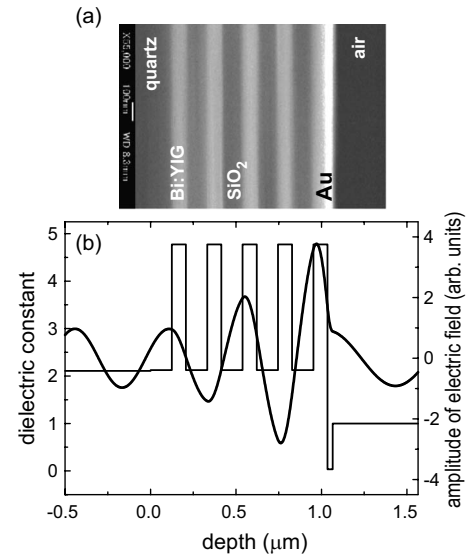


FIG. 4. (a) Scanning electron microscope image of sample 2, the $(\text{SiO}_2/\text{Bi:YIG})^5/\text{Au}$ multilayer. (b) Sketch of the spatial distribution of dielectric constants and the in-sample distribution of the electric field amplitude for the resonant wavelength.

25%. The Faraday rotation for the wavelength of the OTS was found to be enhanced. Spectral widths of the peaks in the spectra of sample 2 were ≈ 40 nm.

Both considered structures were shown to support OTSs and to provide significant enhancement of the MO response of the Bi:YIG constituent layers. Though sample 1 has a more complicated structure, it exhibits the larger transmissivity and Faraday rotation as compared to sample 2. On the other hand, our simulation shows that the calculated magnitudes of the transmittance and of the Faraday rotation for the samples are very close. To understand the difference in the observed enhancement of the Faraday rotation one may consider both samples as resonators in which the Faraday rotation is determined by the quality factor of the transmission resonance. In fact, experimental data show that the peak associated with the OTS for sample 2 is wider than that of sample 1; the quality factor for sample 2 is smaller than that for sample 1. Surely, there are two reasons for the decrease

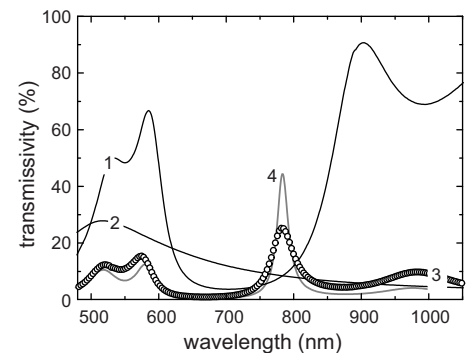


FIG. 5. Transmissivity of the $(\text{Bi:YIG}/\text{SiO}_2)^5$ multilayer and the Au film alone are denoted by (1) and (2), respectively. Transmissivity of sample 2 is shown by circles (3); its calculated spectrum is given by curve (4).

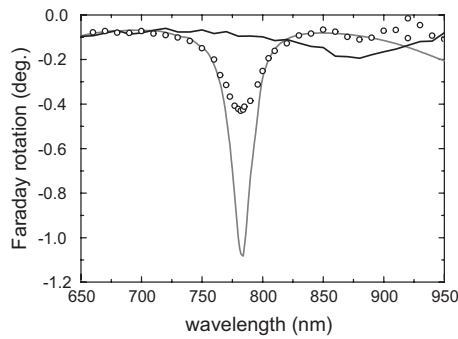


FIG. 6. Angle of Faraday rotation: the $(\text{Bi:YIG/SiO}_2)^5$ multilayer (black solid line), the experimental (circles), and calculated (gray line) spectra of sample 2.

in the quality factor—absorption and structural imperfections in samples. Absorption results in losses of energy of the traveling light; imperfections do the same via diffuse scattering. Figures 1 and 4 show that the accuracy (planarity of layers and fluctuations of the layers' thicknesses) of sample 1 is worse; nevertheless the quality factor for this sample is larger. This means that the OTS is a quite robust phenomenon and that absorption in (and imperfections of) the Au film has larger destructive effect on OTSs.

It is worth mentioning that sample 2 represents the direct optical analog of the conventional crystals supporting the electronic Tamm state while sample 1 resembles the microcavity-type MPC (magnetic Fabry-Pérot microresonator^{4,5}). Despite the simpler structure of sample 2, it is interesting not only from the fundamental point of view. A 1D photonic structure^{14,27} with the last layer made of a noble metal and/or attached to it any other active material supporting additional resonances or transitions can provide a very sensitive element for probing properties of biomolecules and bioreactions.

IV. CONCLUSION

We have demonstrated that tailoring surfaces and interfaces of PCs can provide conditions for the existence of OTSs. These states manifest themselves as resonant peaks in transmission and Faraday rotation spectra of MPCs. Indeed, in the magnetophotonic structures that we discussed, both the Faraday rotation angle, θ_F , and the transmission coefficient, T , are large at the resonant frequency. Therefore, the magneto-optical quality factor, $\theta_F/\ln T$, is substantially greater than can be achieved in homogeneous magneto-optical material. Owing to these characteristics, MPCs supporting OTSs can be used for magnetotunable filters.¹¹

Structures exhibiting OTSs can be useful for localizing light within any active material used as the constitutive layers of PCs or introduced at the interface between two PCs. OTSs can provide an additional mechanism to increase the surface electric field strength in photonic structures called upon to excite long-range surface-plasmon polaritons.^{14,27} For such structures (sample 2 in our work), which are attractive for sensing applications, spectral characteristics of OTSs may have a strong response to a change in dielectric conditions in the vicinity of open surfaces.

ACKNOWLEDGMENTS

The work at TUT was supported in part by Grant-in-Aid for Scientific Research (S) No. 17106004 from Japan Society for the Promotion of Science (JSPS) and the Super Optical Information Memory Project from the Ministry of Education, Culture, Sports, Science and Technology of Japan (MEXT). This work was also supported by the Global COE Program "Frontiers of Intelligent Sensing" from the Ministry of Education, Culture, Sports, Science and Technology of Japan (MEXT). Authors at ITAE and MSU acknowledge support by RFBR under Grants No. 08-02-00874 and No. 07-02-91583. A.L. acknowledges support by AFSOR under Grant No. FA9550-07-1-0391.

¹J.-M. Lourtioz, H. Benisty, V. Berger, J.-M. Gerard, D. Maystre, and A. Tchernikov, *Photonic Crystals: Towards Nanoscale Photonic Devices* (Springer, Berlin, 2005).
²J. D. Joannopoulos, R. Meade, and J. Winn, *Photonic Crystals* (Princeton University Press, Princeton, NJ, 1995).
³K. Sakoda, *Optical properties of Photonic Crystals* (Springer, Berlin, 2001).
⁴M. Inoue and T. Fujii, *J. Appl. Phys.* **81**, 5659 (1997).
⁵M. Inoue, R. Fujikawa, A. Baryshev, A. Khanikaev, P. B. Lim, H. Uchida, O. Aktsipetrov, A. Fedyanin, T. Murzina, and A. Granovsky, *J. Phys. D* **39**, R151 (2006).
⁶M. Levy and R. Li, *Appl. Phys. Lett.* **89**, 121113 (2006).
⁷M. Levy and A. A. Jalali, *J. Opt. Soc. Am. B* **24**, 1603 (2007).
⁸S. Kahl and A. M. Grishin, *Appl. Phys. Lett.* **84**, 1438 (2004).
⁹S. I. Khartsev and A. M. Grishin, *J. Appl. Phys.* **101**, 053906 (2007).
¹⁰A. P. Vinogradov, A. V. Dorofeenko, S. G. Erokhin, M. Inoue, A. A. Lisyansky, A. M. Merzlikin, and A. B. Granovsky, *Phys.*

Rev. B **74**, 045128 (2006).

¹¹A. M. Merzlikin, A. P. Vinogradov, A. V. Dorofeenko, M. Inoue, M. Levy, and A. B. Granovsky, *Physica B* **394**, 277 (2007).
¹²A. Kavokin, I. Shelykh, and G. Malpuech, *Appl. Phys. Lett.* **87**, 261105 (2005).
¹³M. Kaliteevski, I. Iorsh, S. Brand, R. A. Abram, J. M. Chamberlain, A. V. Kavokin, and I. A. Shelykh, *Phys. Rev. B* **76**, 165415 (2007).
¹⁴M. E. Sasin, R. P. Seisyan, M. A. Kaliteevski, S. Brand, R. A. Abram, J. M. Chamberlain, A. Yu. Egorov, A. P. Vasil'ev, V. S. Mikhlin, and A. V. Kavokin, *Appl. Phys. Lett.* **92**, 251112 (2008).
¹⁵C. R. Rosberg, D. N. Neshev, Y. V. Kartashov, R. A. Vicencio, W. Krolikowski, M. I. Molina, A. Mitchell, V. A. Vysloukh, L. Torner, and Yu. S. Kivshar, *Opt. Photonics News* **17**, 29 (2006).
¹⁶N. Malkova and C. Z. Ning, *Phys. Rev. B* **73**, 113113 (2006).
¹⁷N. Malkova and C. Z. Ning, *Phys. Rev. B* **76**, 045305 (2007).
¹⁸A. Figotin and I. Vitebskiy, *Phys. Rev. B* **77**, 104421 (2008).

- ¹⁹I. E. Razdol'skii, T. V. Murzina, O. A. Aktsipetrov, and M. Inoue, *Pis'ma Zh. Eksp. Teor. Fiz.* **87**, 461 (2008) [*JETP Lett.* **87**, 395 (2008)].
- ²⁰P. Sheng, *Introduction to Wave Scattering, Localization, and Mesoscopic Phenomena* (Academic, London, 1995).
- ²¹T. Goto, A. V. Dorofeenko, A. M. Merzlikin, A. V. Baryshev, A. P. Vinogradov, M. Inoue, A. A. Lisyansky, and A. B. Granovsky, *Phys. Rev. Lett.* **101**, 113902 (2008).
- ²²I. Y. Tamm, *Phys. Z. Sowjetunion* **1**, 733 (1932).
- ²³W. Shockley, *Phys. Rev.* **56**, 317 (1939).
- ²⁴M. Komiyama, *Kogakuhakumaku no Kisoriron* [Optronikusu Publishing Inc. (in Japanese), Tokyo, 2003].
- ²⁵E. D. Palik, *Handbook of Optical Constants of Solids* (Academic, New York, 1985).
- ²⁶Optical constants for Bi:YIG were evaluated by a J. A. Woollam Co. ellipsometer.
- ²⁷V. N. Konopsky and E. V. Alieva, *Phys. Rev. Lett.* **97**, 253904 (2006).